Performance Characteristics of the Series Hybrid Electric Vehicle with Hybrid Mode

Ibrahim A.M. Abdel-Halim, Mohsen Z. Elsherif and Mohamed M. Fathy
Faculty of Engineering (Shoubra), Benha University, 108, Shoubra Street, Cairo, Egypt

Abstract: In this study, the equations describing the performance of the series hybrid electric vehicle are derived. Performance characteristics for each part in the vehicle system are obtained when the vehicle is operating in hybrid mode in which the drive motor takes its power from main and peaking power sources.

Key words: Induction motor, electric vehicle, hybrid electric vehicle, hybrid mode

INTRODUCTION

Hybrid Electric Vehicles (HEVs) contain two energy sources to propel the vehicle. One of these energy sources is mechanical which is an Internal Combustion Engine (ICE) and the other is an energy storage device which can be electrochemical batteries (Assanis *et al.*, 1999; Merkle, 1997; Ciccarelli and Toossi, 2002). Thus, the hybrid electric vehicle is a hybrid between the conventional vehicle, ICE vehicle and the pure Electric Vehicle (EV) so that it can take merits and overcome problems concerned with these two types of vehicles.

According to the orientation of the two energy sources in the propulsion system, there are two common configurations of hybrid electric vehicles which are the series and parallel configuration (Assanis *et al.*, 1999; Merkle, 1997; Ciccarelli and Toossi, 2002; Farrell *et al.*, 1998). The series HEVs only have an electric propulsion

system coupled to the wheels and there is no mechanical connection between the internal combustion engine and the wheels axle. The power for the electric propulsion system comes from the energy storage device and/or an electric generator which is coupled to the internal combustion engine. The internal combustion engine and the generator are normally used for highway driving while the peaking power source provides added power during acceleration, hill climbing and other periods of high power demand (Ciccarelli and Toossi, 2002). This mode of operation in which both power sources are used to feed the drive motor is the hybrid mode of operation. In this study, it will be assumed that the energy storage device (the peaking power source) used is a bank of electrochemical batteries and the performance of the series HEV in the hybrid mode is investigated. The system of the series HEV investigated is shown in Fig. 1. This
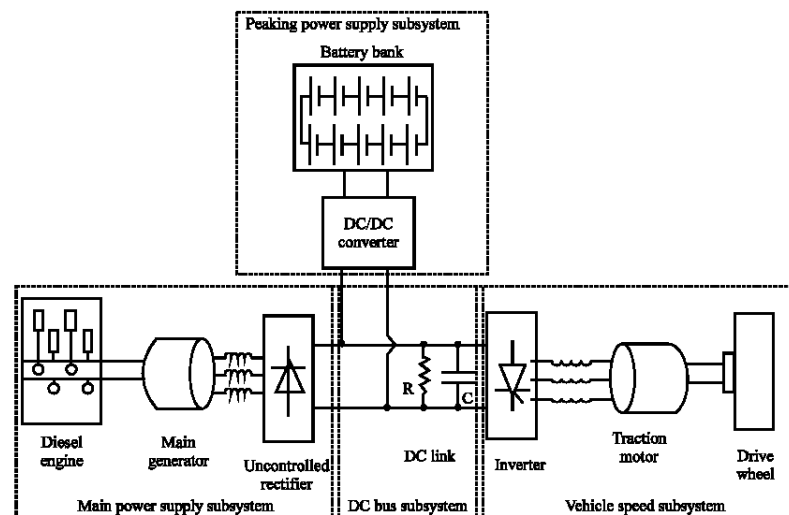

Fig. 1: The series HEV system

Corresponding Author: Ibrahim A.M. Abdel-Halim, Faculty of Engineering (Shoubra), Benha University, 108, Shoubra Street, Cairo, Egypt

system consists of four main subsystems which are the main power supply subsystem, the peaking power supply subsystem (the energy storage system), the vehicle speed subsystem and the DC bus subsystem.

MATERIALS AND METHODS

Performance equations of the series HEV with hybrid mode: This mode of operation of the series HEV may be used when a large amount of power is demanded such as during sharp acceleration or steep hill climbing. In this mode, the electric motor drive takes its power from both the main and peaking power sources.

To investigate the series HEV performance at acceleration. It will be assumed that the vehicle is accelerated with the drive motor is fed from a variable-voltage, variable-frequency source with its air-gap flux is kept constant at the value corresponding to fundamental frequency. The tractive force developed at the shaft of the wheel axle during acceleration can be expressed by:

$$F_{TR} = K_m M_{veh} \frac{dV_{veh}}{dt} + F_{RL} \qquad (1)$$

Where:

$$F_{RL} = C_0 M_{veh} g + 0.5 \rho C_D A_f V_{veh}^2$$

Therefore, the acceleration of the vehicle can be expressed by:

$$\frac{dV_{veh}}{dt} = \frac{1}{k_m M_{veh}} (F_{TR} - F_{RL}) \qquad (2)$$

Thus, the torque at the shaft of the wheel axle can be expressed by:

$$T_{wh} = (C_0 M_{veh} g + 0.5 \rho C_D A_f V_{veh}^2) r_{wh} + T_b \qquad (3)$$

The developed power at the shaft of the wheel axle can be determined from:

$$P_{wh} = T_{wh} \frac{V_{veh}}{r_{wh}} \qquad (4)$$

The motor speed can be expressed in terms of the vehicle speed as:

$$\omega_m = m \frac{V_{veh}}{r_{wh}} \qquad (5)$$

Where m is the gear ratio of the mechanical coupling between the induction motor and the axle of the vehicle wheels. Therefore, the motor torque is expressed by:

$$T_{im} = \frac{P_{wh}}{\eta_{tmw} \omega_m} \qquad (6)$$

or by;

$$T_{im} = \frac{T_{wh}}{\eta_{tmw} \omega_m} \frac{V_{veh}}{r_{wh}} \qquad (7)$$

Where η_{tmw} is the efficiency of the transmission between the traction motor and the wheel axle. The corresponding tractive force will be:

$$F_{TR} = \frac{T_{im} \eta_{tmw} \omega_m}{V_{veh}} \qquad (8)$$

Substituting from Eq. 5 into 6, the motor torque can be expressed in terms of the vehicle speed as:

$$T_{im} = \frac{P_{wh} r_{wh}}{\eta_{tmw} m V_{veh}} \qquad (9)$$

The DC bus power can be expressed by:

$$P_{bus} = \frac{P_{m\_in}}{\eta_{mc}} \qquad (10)$$

Where η_{mc} is the efficiency of the converter. At stand still the motor developed torque is related to the torque at the shaft of the wheel axle by the relationship:

$$T_{whst} = m T_{imst} \qquad (11)$$

The corresponding tractive force will thus be:

$$F_{TRst} = \frac{T_{whst}}{r_{wh}} \qquad (12)$$

Algorithm for obtaining results: Starting from zero vehicle speed, the motor speed would be equal to zero. Then using the motor equivalent circuit shown in Fig. 2 at known voltage and frequency, the developed torque of the induction motor at standstill, T_{imst} can be obtained. The corresponding tractive force, F_{TRst} can thus, be obtained from Eq. 12.

Using this value of tractive force into Eq. 2, the next vehicle speed can be obtained by integrating this equation numerically over an appropriate time step. For the second and following time steps of numerical solution, the corresponding motor speed is obtained from Eq. 5 and the motor equivalent circuit is used to obtain its developed torque and the corresponding tractive force is obtained from Eq. 8. This process continues until the vehicle reaches steady-state speed.
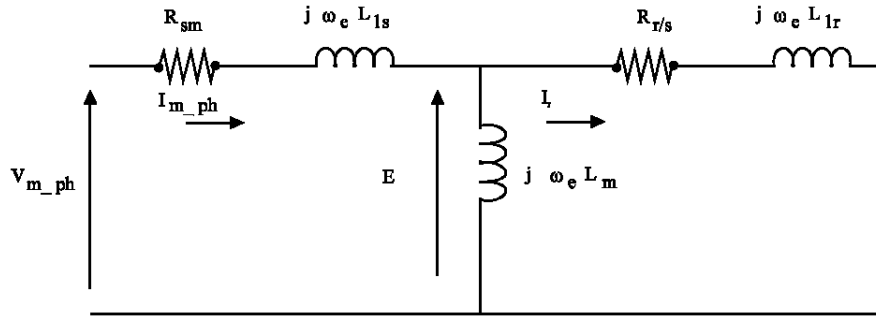
Fig. 2: Equivalent circuit of the induction motor

RESULTS AND DISCUSSION

The approach shown in Eq. 3 was applied using 4th order Runge-Kutta numerical method of integration with the air-gap flux of the motor kept constant. Several performance characteristics of the vehicle during acceleration at different voltage and frequency of the motor using the data of the induction motor and vehicle shown in Appendix 1 are obtained.

Figure 3 shows the variation of the vehicle speed throughout the acceleration period. From Fig. 3, it is clear that the vehicle reaches a higher final steady-state speed as the motor voltage and frequency increases. The tractive and resisting forces, F_{TR} and F_{RL}, respectively are plotted against time during acceleration and until steady state conditions are reached at the same values of the voltage and frequency used to obtain Fig. 3 as shown in Fig. 4-7. From these, it is clear that as the voltage and frequency increases the vehicle will take a shorter time to accelerate to steady-state speed.

The tractive and resisting forces, F_{TR} and F_{RL} can also be drawn against the vehicle speed during the acceleration period until steady-state conditions are reached for different values of motor voltage and frequency, as shown in Fig. 8-11. From Fig. 8-11, it is clear that for certain voltage and frequency values, the tractive force decreases and the resisting force increases as the vehicle speed increases up to steady-state speed at which the tractive and resisting forces are equal. For a certain vehicle speed, the tractive force decreases while the resisting force is constant for the several values of voltage and frequency used when their values decrease. Using the values of the vehicle speed which are obtained at different values of motor voltage and frequency into Eq. 3, the characterisitics of the torque at the wheel axle, T_{wh} can be drawn versus the vehicle speed during acceleration until steady-state conditions are reached as shown in Fig. 12. From Fig. 12, it is noticed that the torque applied on the wheel axle has the same shape as that of the corresponding tractive force shown in Fig. 8-11
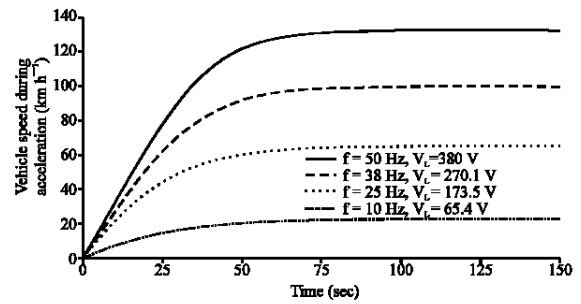

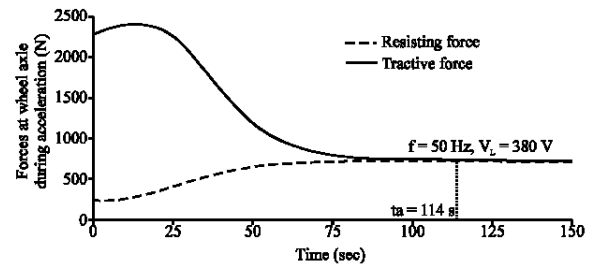Fig. 3: Vehicle speed versus time during acceleration

Fig. 4: Tractive and resisting forces at wheel axle versus time (f = 50 Hz, V_L = 380 V)

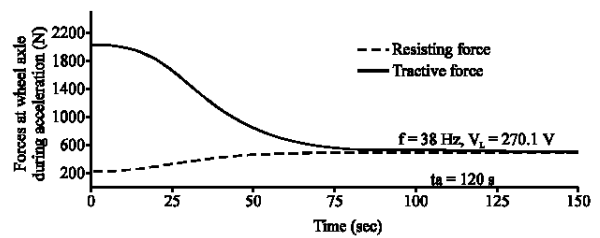Fig. 5: Tractive and resisting forces at wheel axle versus time (f = 38 Hz, V_L = 270.1 V)

and for the same vehicle speed the torque decreases as the used values of the voltage and frequency decrease. From Eq. 4, the characterisitics of the developed power at the wheel axle can be obtained against time and against the vehicle speed at different values of the motor voltage
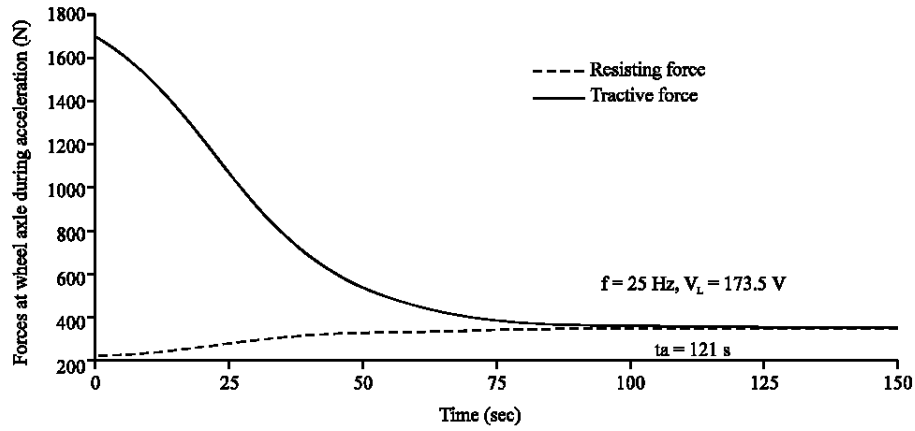
Fig. 6: Tractive and resisting forces at wheel axle versus time (f = 25 Hz, V_L = 173.5 V)
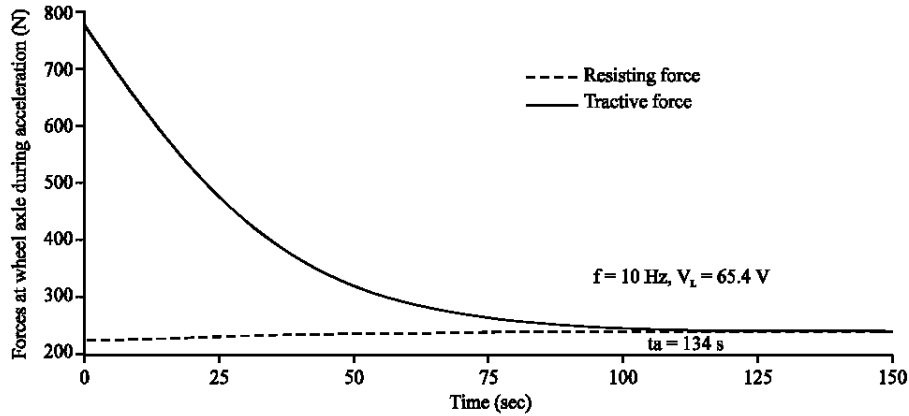

Fig. 7: Tractive and resisting forces at wheel axle versus time (f = 10 Hz, V_L = 65.4 V)

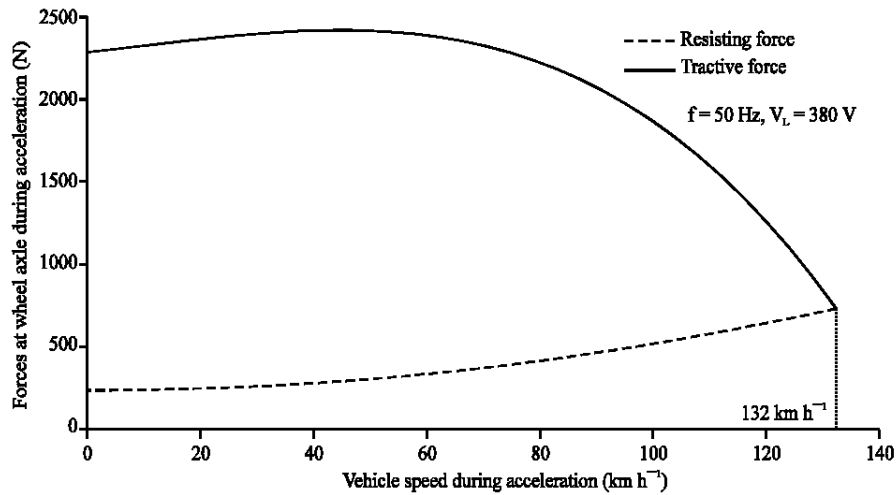Fig. 8: Tractive and resisting forces at wheel axle versus vehicle speed during acceleration (f = 50 Hz, V_L = 380 V)

and frequency as shown in Fig. 13 and 14, respectively. From Fig. 13, it is clear that at certain values of voltage and frequency, the developed power at the wheel axle increases until it reaches a maximum value and then decreases as the time increases until the vehicle reaches steady-state speed at which the developed power
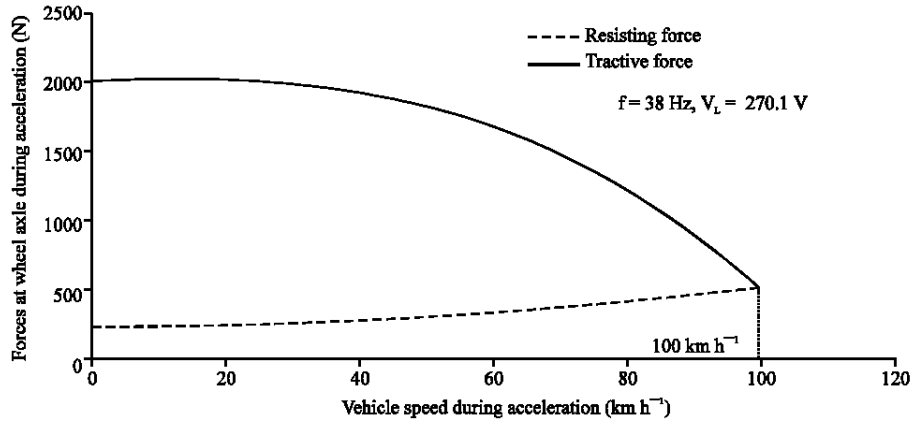
99

Fig. 9: Tractive and resisting forces at wheel axle versus vehicle speed during acceleration (f = 38 Hz, V_L = 270.1 V)
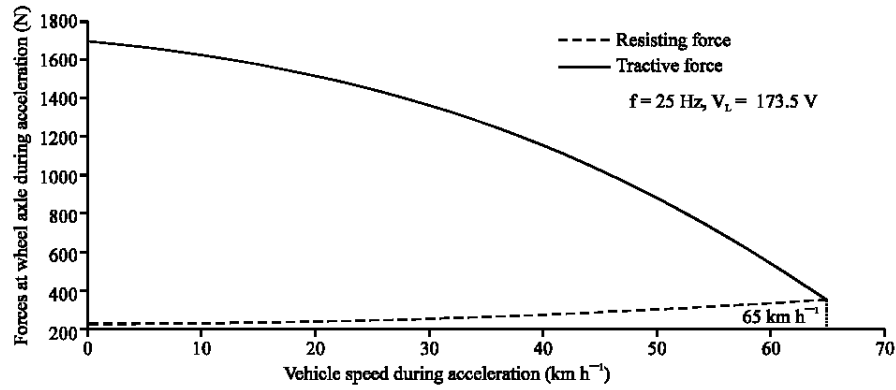

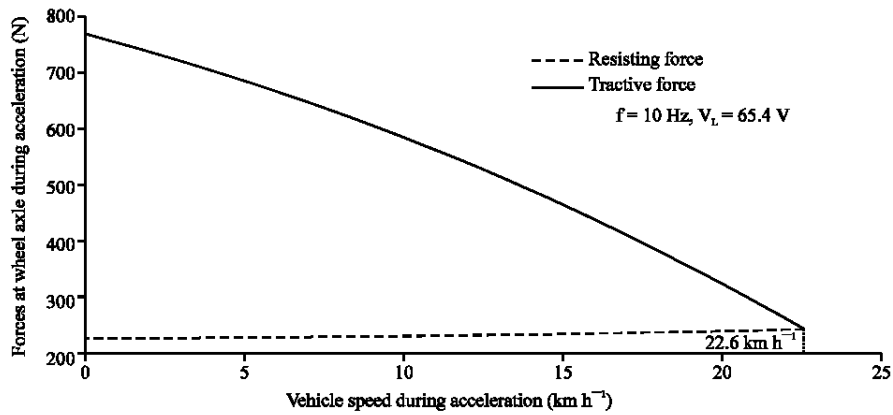Fig. 10: Tractive and resisting forces at wheel axle versus vehicle speed during acceleration (f = 25 Hz, V_L = 173.5 V)

Fig. 11: Tractive and resisting forces at wheel axle versus vehicle speed during acceleration (f = 10 Hz, V_L = 65.4 V)

becomes constant. Also, at any instant of time the developed power has higher values at higher voltages and frequencies. From Fig. 14 for certain values of motor voltage and frequency, the developed power at the wheel axle increases to a maximum value and then decreases as the vehicle speed increases. Also, at certain vehicle speed the developed power has higher values at higher voltages and frequencies and the vehicle speed, at which the developed power on the wheel axle will have a maximum value is increasing as the motor voltage and frequency
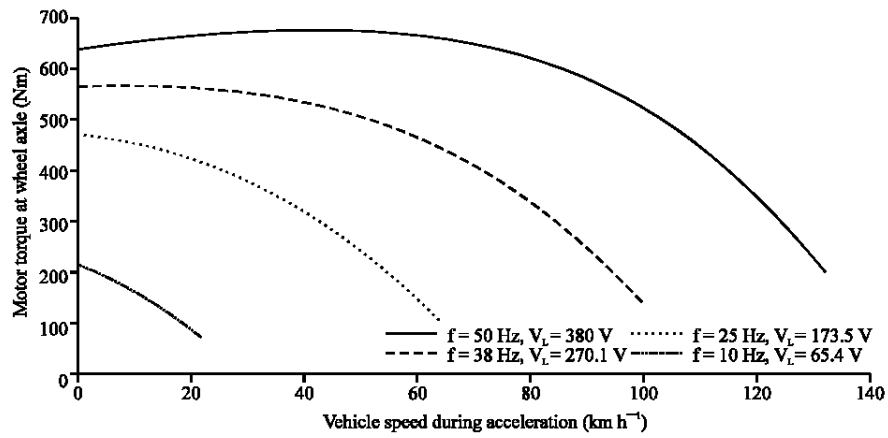
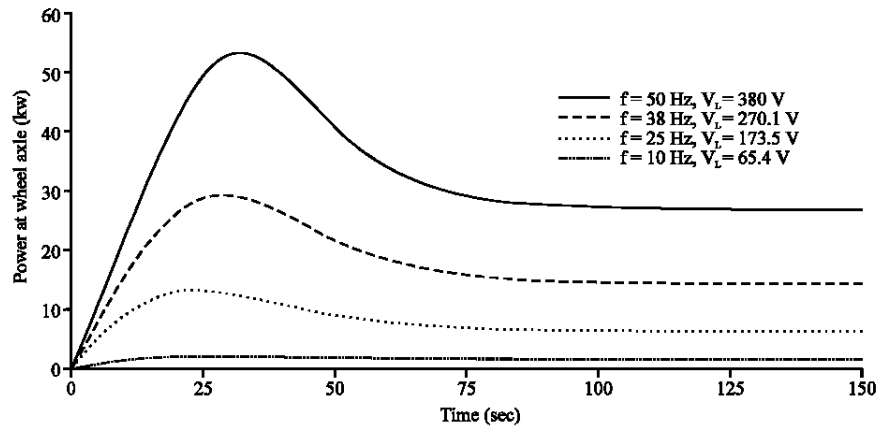Fig. 12: Torque applied on wheel axle versus vehicle speed

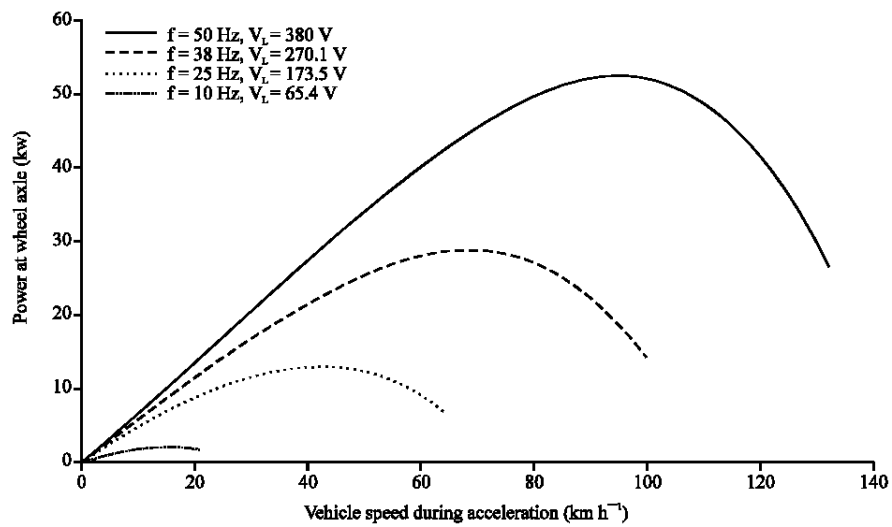Fig. 13: Developed power at wheel axle versus time

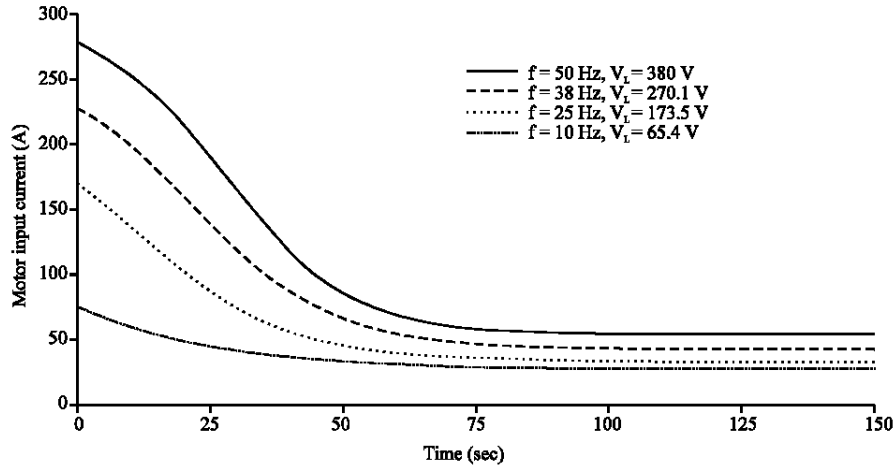Fig. 14: Developed power at wheel axle versus vehicle speed

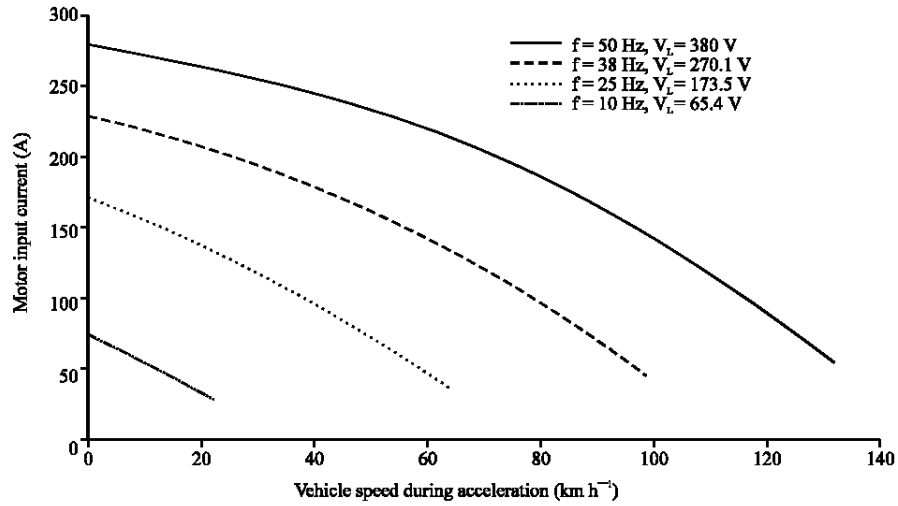Fig. 15: Motor input current versus time

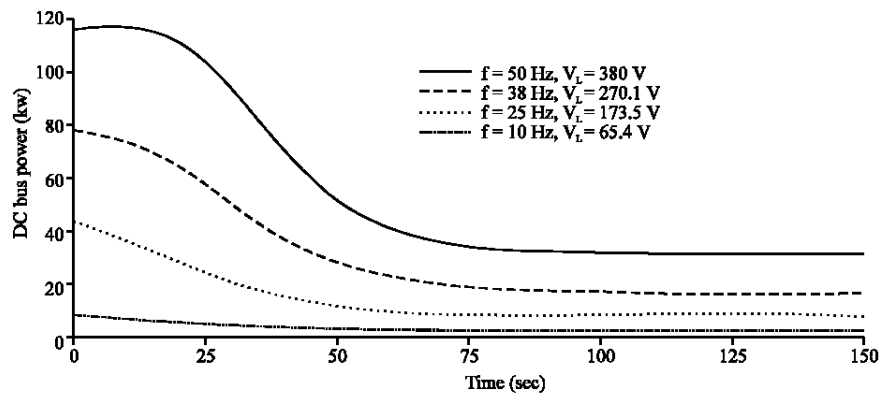Fig. 16: Motor input current versus vehicle speed during acceleration

Fig. 17: DC bus power versus time during acceleration

increases. From Eq. 9, the motor torque can be calculated at different values of the vehicle speed. Then, using these values of the motor torque into the motor equivalent circuit shown in Fig. 2, the motor input current can be
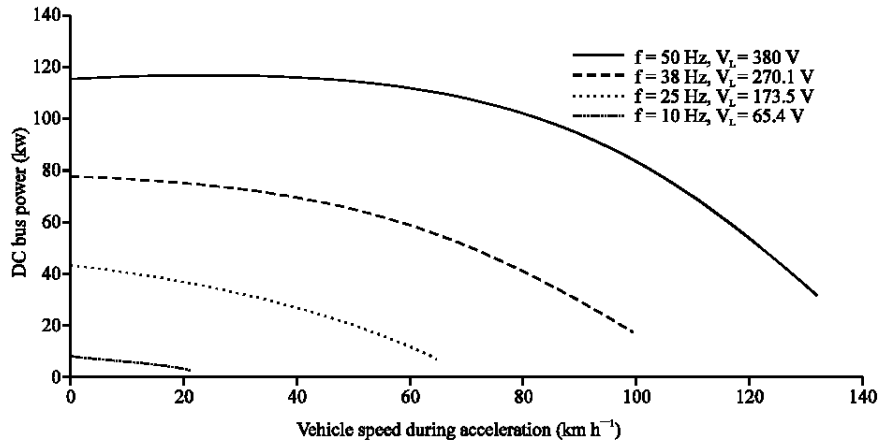
Fig. 18: DC bus power versus vehicle speed during acceleration

determined and ploted against time and against vehicle speed, for different values of voltages and frequencies as shown in Fig. 15 and 16, respectively. From Fig. 15 and 16, it is clear that at certain values of voltage and frequency, the motor input current decreases as the vehicle accelerates and reaches a constant rms value at steady state. For any time instant (Fig. 15) or vehicle speed (Fig. 16) the motor input current will have larger values for higher values of voltage and frequency.

Determining the motor input current and power factor at different values of the motor voltage and frequency, the motor input power, P_{m_in} can be also computed. Using the different values of the computed motor input power at different values of the motor voltage and frequency into Eq. 10, the DC bus power can be obtained during the acceleration period as shown in Fig. 17 and 18, respectively. From these, it is clear that at a constant voltage and frequency, the DC bus power decreases as the vehicle accelerates and then at a constant vehicle speed the DC bus power decreases as the voltage and frequency decreases.

CONCLUSION

From the performance characteristics of the series HEV operating in the hybrid mode, the following is observed as the motor voltage and frequency increases:

- The vehicle reaches a higher final steady-state speed
- The vehicle will take a shorter time to accelerate to steady-state speed
- The tractive force increases while the resisting force is constant for a certain vehicle speed
- The motor torque increases for a certain vehicle speed
- The developed power has higher values at certain vehicle speed or at any instant of time

- The motor input current will have larger values for any time instant or vehicle speed
- The DC bus power increases at a constant vehicle speed

Also for certain operating values of the motor voltage and frequency:

- The tractive force decreases and the resisting force increases as the vehicle speed increases up to steady-state speed at which the tractive and resisting forces are equal
- The developed power at the wheel axle increases until it reaches a maximum value and then decreases as the time increases until the vehicle reaches steady-state speed at which the developed power becomes constant
- The motor input current decreases as the vehicle accelerates and reaches a constant rms value at steady state
- The DC bus power decreases as the vehicle accelerates

List of symbols:

A_f	=	Equivalent frontal area of the vehicle in m^2
C_0	=	Coefficient of rolling resistance
C_D	=	Aerodynamic drag coefficient
F_{RL}	=	Road load force in N
F_{TR}	=	Tractive force in N
g	=	Gravitational acceleration constant in m sec^{-2}
k_m	=	Rotational inertia coefficient
m	=	Gear ratio of the gear box
M_{veh}	=	Total mass of the vehicle in kg
P_{bus}	=	Input DC bus power in W
P_{wh}	=	Power at the shaft of the wheel axle in W
P_{m_in}	=	Input power of the induction motor in W
r_{wh}	=	Radius of the wheel in m

T_b	=	Frictional brake torque in Nm
T_{im}	=	Developed torque of the induction motor in Nm
T_{wh}	=	Load torque at the shaft of the wheel axle in Nm
V_{veh}	=	Vehicle speed in km h^{-1}
γ	=	Grade angle
η_{mc}	=	Efficiency of the motor converter
η_{tmw}	=	Efficiency of transmission between the traction motor and the wheel axle
ρ	=	Air density in kg m^{-3}
ω_m	=	Motor speed in rad sec^{-1}

APPENDIX

Data of the induction motor: P_{mr} = 41.3 kW, V_{mr} = 380 V, f_r = 50 Hz, star connected 3-phase induction motor, n_r = 1230 rpm, s_r = 0.18, P = 4 poles, η_{in} = 0.85, R_{sm} = 0.0862 ohm, R_r = 0.427 ohm, L_m = 0.029974 H, L_{ls} = L_{lr} = 9.761503×10^{-4} H.

Vehicle dynamic parameters: ρ = 1.225 kg m^{-3}, C_D = 0.3, A_f = 2 m^2, M_{veh} = 2250 kg, r_{wh} = 0.2794 m, Tb = 0, $V_{veh-max}$ = 120 km h^{-1}, V_f = 100 km h^{-1}, km = 1.08, C_0 = 0.01, g = 9.81 m sec^{-2}, m = 1.1, η_{mc} = 0.98, η_{tmw} = 0.95, R_{bus} = 510.

REFERENCES

Assanis, D., G. Delagrammatikas, R. Fellini, Z. Filipi and J. Liedtke *et al.*, 1999. An optimization approach to hybrid electric propulsion system design. Mech. Struct. Mach., 27: 393-421.

Ciccarelli, T. and R. Toossi, 2002. Assessment of hybrid configuration and control strategies in planning future metropolitan/urban transit systems. Final Report, California State University, pp: 1-63. http://www.metrans.org/research/final/00-06_Final. pdf.

Farrell, J.A., M.J. Barth and J.W. Heffel, 1998. Hydrogen-powered advanced hybrid-electric vehicles. Final Report, College of Engineering Center for Environmental Research and Technology University of California, pp: 1-101.

Merkle, M.A., 1997. Variable bus voltage modeling for series hybrid electric vehicle simulation Master Thesis, Virginia Polytechnic Institute and State University, Blacksburg, Virginia.